

## Recent advances in the energetics and mechanisms of gas-phase ionic reactions

José M. Riveros\*, Marcelo Sena, Gustavo H. Guedes, Luciano A. Xavier, and Roberto Slepetyś F.

*Institute of Chemistry, University of São Paulo, Caixa Postal 26077, São Paulo, Brazil, CEP 05599-970.*

**Abstract:** Three important aspects are still at the forefront of gas-phase ion chemistry: structure and energetics, mechanisms of gas-phase reactions relevant to condensed phases, and bridging the gap between gas-phase and solution. In this paper, we review some recent results of our laboratories: 1) The use of incoherent infrared radiation to promote multiphoton dissociation of ions is shown to be an efficient and convenient method to determine the energetics of ions and provide structural information of ions. 2) New experimental and theoretical data provide some interesting comparison between nucleophilic reactions at carbon, silicon and germanium centers. In the latter cases, the mechanism involves primarily an attachment-detachment process. 3) The ability to make gas-phase anions attached to neutral molecules provides an interesting approach towards the study of the stability, reactivity, structure and spectroscopy of gas-phase solvated ions.

### INTRODUCTION

Gas-phase ion chemistry has contributed in remarkable ways towards our understanding of the intrinsic properties and reactivity of simple organic compounds in the last 30 years. The continuous refinement of experimental techniques has increasingly expanded the horizon of gas-phase ion chemistry, and considerable effort is being directed towards bridging the gap between chemical behavior in the low-pressure gaseous regime and that observed under bulk solvent conditions. Ion chemistry has also derived immense benefits from a rich interplay between experimental and computational chemistry, and few areas of chemistry can probably rival the synergism between theory and experiment.

In this contribution, we will review three topics presently under investigation in our laboratories and that are relevant to three important aspects of physical organic chemistry: 1) the thermochemical parameters of ions; 2) the mechanism of simple ionic reactions; and 3) gas-phase ion solvation and its relationship with condensed phase chemistry. While our work has used primarily ion cyclotron resonance techniques (Ref. 1), relevant information on these three subjects can be obtained by a combination of mass spectrometric methods (Ref. 2).

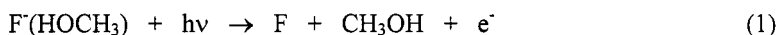
### DISSOCIATION TECHNIQUES AND THERMOCHEMISTRY OF IONS

One of the most important areas of gas-phase ion chemistry has been the quest for thermodynamic parameters associated with ions: heats of formation, proton affinities, and binding energies of gas-phase ion-neutral complexes resembling solvated ions. These quantities are essential for understanding the energetics of chemistry. Furthermore, there is a growing number of elusive neutral species that can be characterized thermodynamically from ion-related experiments.

---

\*Lecture presented at the 14th International Conference on Physical Organic Chemistry, Florianópolis, Brazil, 21–26 August 1998. Other presentations are published in this issue, pp. 1933–2040.

One approach that can be used to obtain relevant thermochemical data relies on measuring photodissociation thresholds by photon impact. For example, the binding energy of the gas-phase  $F^-$  (HOMe) cluster ion has been determined to be  $126 \text{ kJ mol}^{-1}$  from the threshold wavelength for the photodetachment process shown in equation 1 (Ref. 3).



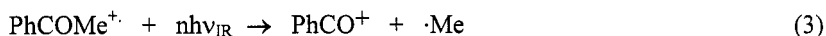
Unfortunately, extracting accurate binding energies from these experiments generally requires some knowledge about the electronic states of the photofragmentation products.

An interesting and different approach to ion photodissociation was demonstrated recently and relies on the use of broadband incoherent infrared radiation. For example, weakly bound ionic complexes trapped in the cell of an FTICR spectrometer are observed to undergo facile unimolecular dissociation (equation 2) under the combined effects of the background blackbody radiation and the stray light from the weakly incandescent filament used for producing the ions (Ref. 4).



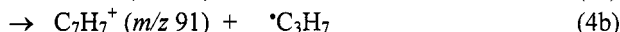
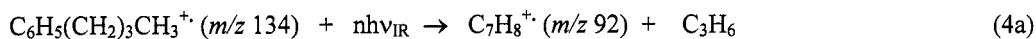
This observation is similar to the first reports describing the dissociation of weakly bound cluster ions by blackbody radiation (Ref. 5). Several examples have been illustrated in the literature of this phenomenon (Ref. 6), and dissociation energies for ionic species can be obtained from the temperature dependence of the dissociation rate constant (Ref. 7).

One particular disadvantage of blackbody induced dissociation is the fact that these processes are generally very slow. Thus, competition between dissociation and ion/molecule reactions can seriously impair quantitative studies even at very low pressures. Likewise, temperature variation of FTICR cells over a significant range is not experimentally trivial. We have developed a different approach to circumvent these limitations by using a heated tungsten wire installed just outside the FTICR cell. The glow emitted by the tungsten wire closely corresponds to that of a blackbody source with emission characteristics described by an effective blackbody temperature. A full description of this approach has been reported recently and applied to the dissociation of the molecular ion of acetophenone (Ref. 8).



A simulation of this process by an energy random walk model, or by solving an energy grained master equation, yields a dissociation energy of  $80 \text{ kJ mol}^{-1}$  for the acetophenone molecular ion. A large number of substituted acetophenones can be readily dissociated in this fashion and their dissociation energies calculated using this approach.

The actual procedure to obtain dissociation energies can be illustrated for the case of *n*-butylbenzene. The molecular ion of *n*-butylbenzene undergoes photodissociation as shown in equation 4.



The results of a typical experiment are shown in Figure 1 where the fractional dissociation is recorded as a function of the exposure time of the ions to the radiation emitted by the heated tungsten lamp.

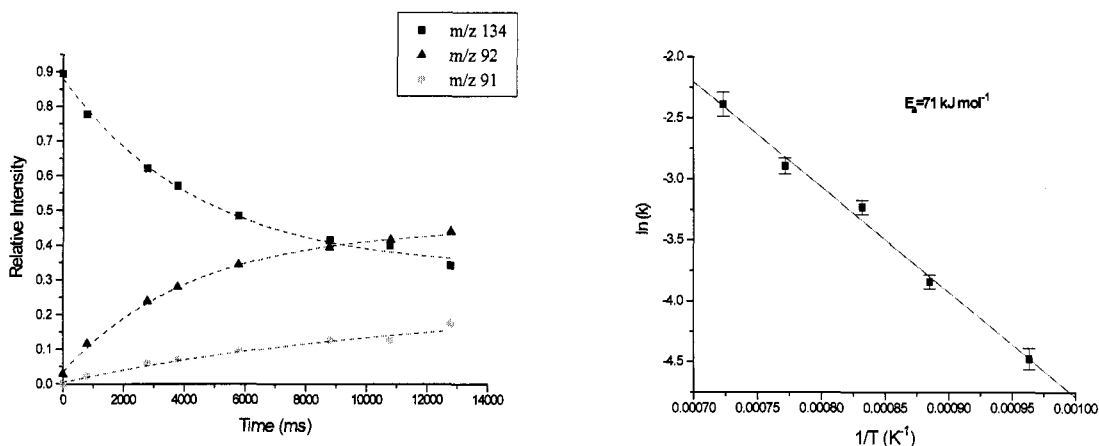
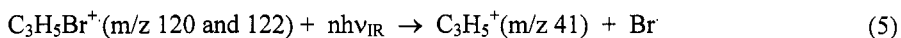


Figure 1: (a) Dissociation of the molecular ion of *n*-butylbenzene as a function of irradiation time with the tungsten lamp emitting 7.3 W of radiation. (b) Activation energy obtained from an Arrhenius plot of the rate constant as a function of the effective blackbody temperature of the lamp.

There are two interesting aspects in this system. Firstly, the relative abundance of the molecular ion approaches a non-zero constant value at long irradiation times. Experiments carried out at different pressures reveal that the  $C_7H_8^+$  ions produced by photodissociation react by charge transfer to regenerate the molecular ion of *n*-butylbenzene. Thus, meaningful experiments had to be performed with *n*-butylbenzene introduced in the ICR cell through a pulsed valve to minimize ensuing ion/molecule reactions. The fact that charge transfer is observed in this situation suggests that the  $C_7H_8^+$  ion produced by photodissociation corresponds to the toluene molecular ion. Secondly, this is one of the few cases in which dissociation is observed to proceed through two channels. Independent experiments with toluene reveal that the molecular ion of toluene does not undergo appreciable dissociation to  $C_7H_7^+$  by incoherent infrared radiation.

The activation energy obtained for the dissociation of *n*-butylbenzene (Figure 1b) is higher than those normally obtained from experiments using near room temperature blackbody radiation. It is this aspect that shows the effectiveness of our method. The dissociation energy for the *n*-butylbenzene molecular ion can then be obtained by using an appropriate master equation approach. This requires knowledge of the vibrational frequencies and the corresponding Einstein absorption and emission coefficients, both of which can be estimated from *ab initio* calculations. An alternative procedure is to use the approximate relationship,  $E_{\text{diss}} \approx E_{\text{act}} + \langle E \rangle - 3.5 \text{ kJ}$  (Ref. 7). A rough estimate of  $\langle E \rangle$ , the average energy of the ions calculated over the reaction depleted internal energy distribution of the reagent ion, yields a dissociation energy of  $\sim 112 \text{ kJ mol}^{-1}$ . While this number is still preliminary, it is very similar to that obtained by other methods (Ref. 9) and refers to the energy required for dissociation to become kinetically measurable.

This dissociation technique can also distinguish isomeric ions in a very elegant way. Two examples are shown in Figure 2. The ionization of allyl bromide is known to give rise to two different molecular ions (Ref. 10). At 20 eV, about 80% of the molecular ions correspond to 3-bromopropene (allyl bromide) radical ion while the other 20% correspond to the 1-bromopropene molecular ion. The 3-bromopropene molecular ions are observed to undergo dissociation under the influence of incoherent infrared radiation as shown below.



By comparison, 1-bromopropene molecular ions do not undergo dissociation presumably due to a much higher dissociation energy. Thus, dissociation continues until all of the 3-bromopropene ion is depleted.

Figure 2b exhibits a similar situation for the molecular ion of 4'-methyl acetophenone. While the keto-form of this ion undergoes dissociation rapidly to yield  $C_8H_7O^+$  ( $m/z$  119), the enol-form is much more stable and exhibits essentially no dissociation.

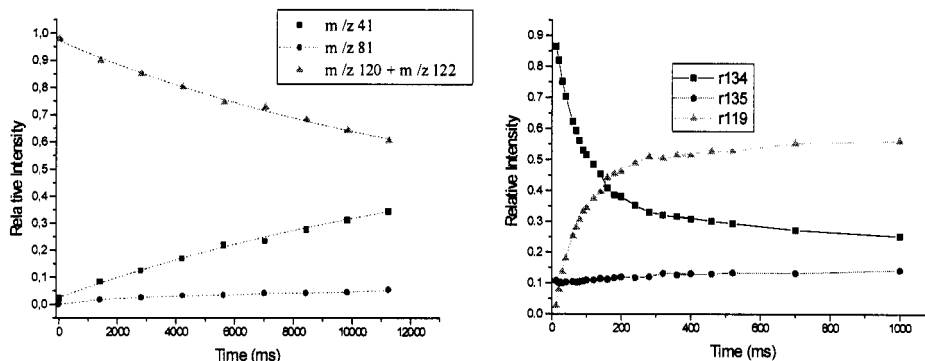
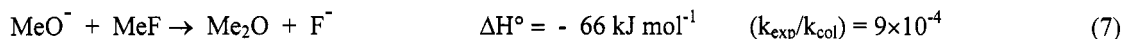
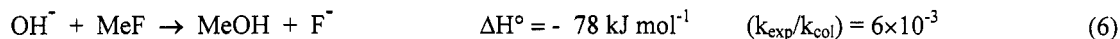


Figure 2: (a) Dissociation kinetics of molecular ion of allyl bromide ( $m/z$  120, 122) to yield  $C_3H_5^+$  ( $m/z$  41) at a lamp power of 7.4 W. A pulsed valve was used to introduce the neutral to avoid ion/molecule reactions ( $C_6H_9^+$ ,  $m/z$  81). (b) Dissociation of the molecular ion of 4'-methyl-acetophenone (pressure  $5.9 \cdot 10^{-8}$  Torr and 10.4 eV electron energy) induced by the in situ lamp operated at 4.35 W. In this experiment, the keto form undergoes dissociation and the enol form promotes no ion/molecule reaction that yields protonated 4'-methyl-acetophenone ( $m/z$  135).

## GAS PHASE NUCLEOPHILIC REACTIONS

### $S_N2$ Reactions

Gas-phase  $S_N2$  reactions have been the center of a great deal of experimental and theoretical research in the last 20 years (Ref. 11). For first row nucleophiles, rate constants for exothermic reactions have been found to be close to the collision rate (Ref. 12). This is not the case for alkyl fluorides in agreement with the common view that  $F^-$  is a poor leaving group. Recent measurements carried out in our laboratories by ICR techniques (at 340 K) show indeed slower rate constants for  $CH_3F$  even though the reactions are substantially exothermic. For example,



A key question in these systems is whether there is an actual activation energy for these reactions. Calculations carried out at the MP2/6-311++G(3dp,3df)//MP2/6-311++G(3dp,3df) level including ZPE (with calculated vibrational frequencies scaled by 0.96) show that the reaction can be described as proceeding through a double well potential (Ref. 10) as outlined in Figure 4.

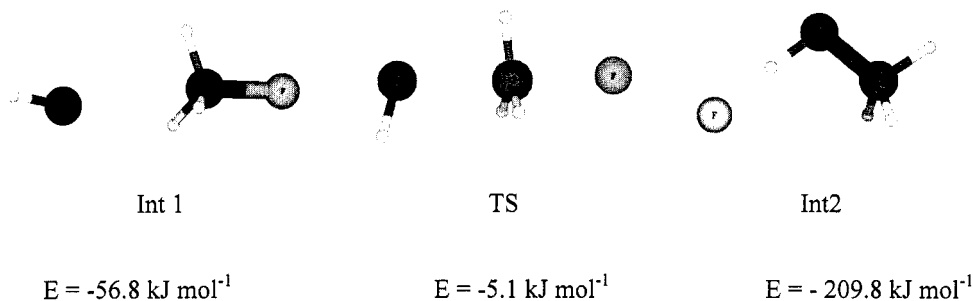


Figure 4: Optimized structures and relative energies (assuming the reagents as  $E = 0$ ) for the intermediates and transition state of reaction (6) calculated at the MP2/6-311++G(3dp,3df)//MP2/6-311++G(3dp,3df) level with ZPE corrections.

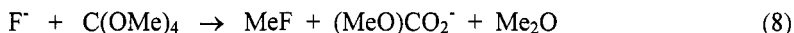
The reaction initially proceeds through the ion-dipole complex **Int 1**, predicted to be  $-56.8 \text{ kJ mol}^{-1}$  below the energy of the reagents, and with a calculated  $\text{HO}^{\cdots}\text{CH}_3\text{F}$  bond of  $2.657 \text{ \AA}$ . The path then proceeds through a Walden-type inversion transition state, **TS**, calculated to be  $-5.1 \text{ kJ mol}^{-1}$  below the energy of the reagents. The structure of this transition state reveals an essentially collinear O-C-F arrangement ( $177.6^\circ$ ) with the  $\text{HO}^{\cdots}\text{C}$  bond length shortened to  $1.974 \text{ \AA}$  while the  $\text{C}^{\cdots}\text{F}$  bond has been elongated to  $1.744 \text{ \AA}$ . The exit channel of this reaction is particularly interesting because no minimum was found for the "reverse"  $\text{S}_{\text{N}}2$  reaction intermediate. As the  $\text{F}^-$  departs, the ion-dipole complex on the product side, **Int 2**, corresponds to that of a  $[\text{F}^{\cdots}\text{HOCH}_3]$  complex, a well known species in the gas phase (Ref. 13). The calculated dissociation energy of this species is calculated to be  $136 \text{ kJ mol}^{-1}$  in good agreement with the experimental value of  $126 \text{ kJ mol}^{-1}$  (Ref. 3), while the overall exothermicity of reaction (6) is calculated to be  $73.9 \text{ kJ mol}^{-1}$ .

The fact that the transition state lies close in energy to that of the reagents is expected to result in a low efficiency for reaction (6). In a naive picture, this is due to the fact that the density of states for the transition state is much lower than that for dissociation back to the reagents. Nevertheless, dynamical effects must be taken into consideration to properly describe gas-phase  $\text{S}_{\text{N}}2$  reactions (Ref. 14).

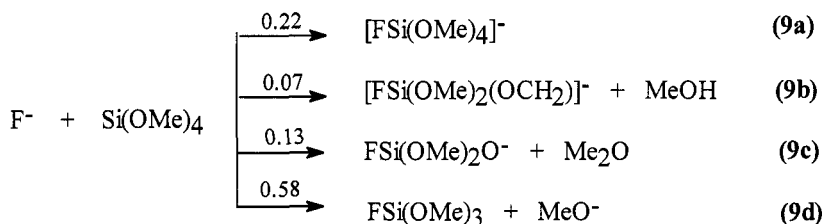
### A Comparison of $\text{S}_{\text{N}}2$ vs Addition Elimination in C, Si and Ge

For a number of years, we have been interested in the competition between  $\text{S}_{\text{N}}2$  reactions and addition-elimination reactions in the gas-phase. For example, we have established that considerable participation of an  $\text{S}_{\text{N}}2$  mechanism is operative in the gas-phase hydrolysis of methyl esters (Ref. 15), and actually becomes the preferred reaction pathway for  $\text{CF}_3\text{COOCH}_3$ . Our investigation has recently been extended to Si and Ge substrates for comparison purposes.

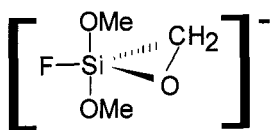
Similar substrates of C, Si and Ge, namely  $\text{M}(\text{OCH}_3)_4$ , were chosen for this purpose due to the interest of the Si and Ge substrates in chemical vapor deposition processes. For the case of  $\text{C}(\text{OMe})_4$ , the gas-phase reaction with  $\text{F}^-$  as the nucleophile reveals very high efficiency and the reaction can be viewed as the result of nucleophilic attack on the methyl group followed by an internal return mechanism (equation 8).



By comparison,  $\text{Si}(\text{OMe})_4$  and  $\text{Ge}(\text{OMe})_4$  display a reactivity that can be explained almost exclusively by addition-elimination mechanisms. For  $\text{Si}(\text{OMe})_4$ , the results are shown in equation 9 (Ref. 16)

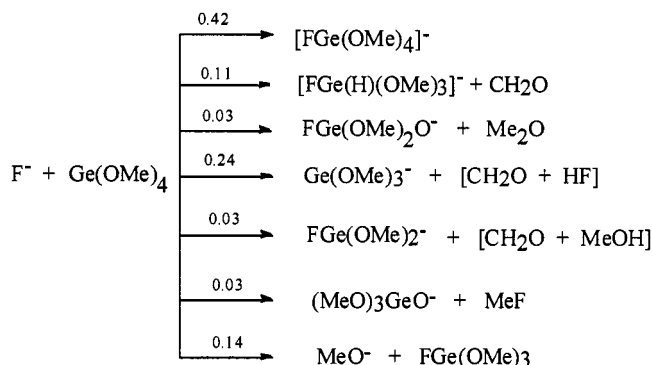


All of the products can be rationalized by an attack of the fluoride ion at the Si center to yield the pentacoordinated adduct,  $\text{FSi}(\text{OMe})_4^-$ , followed by direct elimination of  $\text{MeO}^-$ , or an internal return mechanism to yield the products of reaction (9b) and (9c). Nucleophilic displacement at the Me group to yield  $(\text{MeO})_3\text{SiO}^-$  accounts for less than 3% of the total reaction products.



Theoretical calculations and ion/molecule reactivity of the ion formed in reaction (9b) reveal that this ion corresponds to a silaoxirane structure (Ref. 17), an elusive species which has defied characterization in condensed phases.

Experiments with  $\text{Ge}(\text{OMe})_4$  reveal formal similarities with the Si counterpart but with some significant differences. Formation of the pentacoordinated Ge species is again the main product as in the Si case but the  $\text{FGe}(\text{OMe})_4^-$  undergoes elimination of  $\text{CH}_2\text{O}$  as a primary channel. Furthermore, substituted germyl anions can be generated in this way indicating that these species are more stable than the silicon counterparts. Two other significant results can be pointed out: while formation of a cyclic germaoxirane species cannot be detected in the present experiments (if present it amounts to less than 2% of the reaction products), there is some evidence that at least 3% of the reaction proceeds by  $\text{S}_{\text{N}}2$  displacement at the carbon center.



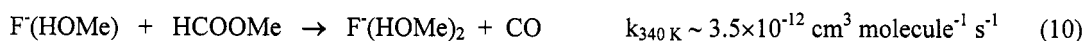
### SOLVATED IONS IN THE GAS PHASE

The ability to form gas-phase ions associated to one or more neutral molecules has been an active area of research since the early 1970's. These gas-phase cluster ions are viewed as mimicking solvated ions. Gas-phase "solvated" anions can be generated by direct association reactions in high pressure mass spectrometers (Ref. 18), indirectly as a result of low pressure bimolecular reactions (Ref. 19), or by electrospray ionization techniques (Ref. 20). For small ions like  $\text{F}^-$  and  $\text{Cl}^-$ , the binding energy between the anion and a single solvent molecule increases with the gas-phase acidity of the neutral substrate (Ref. 21). This trend is preserved even with a large number of solvent molecules around the anion (Ref. 22). For large ions like  $\text{Br}^-$  and  $\text{I}^-$ , ion-dipole interactions can become more important than hydrogen bonding (Ref. 23).

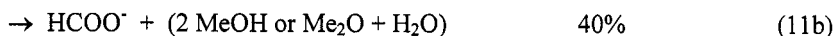
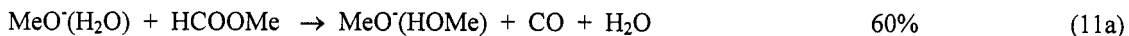
One particular area of interest has been to observe changes in reactivity as a function of anion solvation in the gas-phase (Ref. 24). For example, rate constants for nucleophilic displacement of  $\text{F}^-(\text{H}_2\text{O})_{0-5}$  with  $\text{CH}_3\text{Br}$  decrease significantly with ion solvation (Ref. 25) and become non-measurable by ion chemistry techniques at higher levels of solvation ( $n > 5$ ). By comparison, the rate constant for the proton transfer reaction between  $\text{OH}^-(\text{H}_2\text{O})_{0-11}$  and  $\text{HBr}$  becomes less than the collision limit only after  $n=10$  molecules of solvation (Ref. 26).

We have recently extended our studies on gas-phase solvated anions in two directions: (i) exploring the possibility of generating multiply solvated anions at low pressures, and (ii) developing new spectroscopic methods to study these species.

Reaction of  $\text{F}^-$  with  $\text{HCOOMe}$  is a suitable source of gas-phase  $\text{F}^-(\text{HOMe})$  ions by the so-called "Riveros reaction" (Ref. 13). These ions can undergo a second "Riveros reaction" but with a much slower rate constant to yield a bi-solvated ion (equation 10). Unfortunately, no indication has been observed of tri-solvated  $\text{F}^-$  even after 35 s of ion trapping time.



By comparison, secondary reactions of  $\text{OH}^-$  (obtained from  $\text{H}_2\text{O}$ ) with  $\text{HCOOMe}$  give rise to a mixture of bi-solvated ions such as  $\text{OH}^-(\text{H}_2\text{O})_2$ ,  $\text{MeO}^-(\text{H}_2\text{O})_2$  and  $\text{MeO}^-(\text{MeOH})(\text{H}_2\text{O})$ . Some interesting changes in reactivity are observed upon solvation. For example  $\text{MeO}^-$  reacts with  $\text{HCOOMe}$  to yield almost exclusively the solvated ion  $\text{MeO}^-(\text{HOMe})$  and less than 5% of  $\text{HCOO}^-$ . By comparison, reaction of  $\text{MeO}^-(\text{H}_2\text{O})$  with  $\text{HCOOMe}$  changes dramatically the product distribution.



Aside from changes in reactivity, the structure of solvated anions in the gas phase is of particular interest. One of the key questions is to know whether gas-phase solvated ions display a shell structure resembling bulk solution behavior. Evidence based on IR spectra of  $\text{Br}^-(\text{H}_2\text{O})_n$  suggests that up to  $n = 6$ , the  $\text{Br}^-$  ion solvates on the surface of a strong cyclic water molecule network (27). We have developed an alternative method to study the IR spectra of  $\text{Br}^-$  solvated ions in the gas-phase. This method relies on formation of clusters  $\text{Br}^-(\text{HOR})$  from exchange reactions (23) in the ICR cell. Isolation of these ions in the ICR cell followed by irradiation with a  $\text{CO}_2$  laser results in facile photodissociation by a sequential absorption of 3 or 4 infrared photons. This approach leads to a partial IR spectra of the solvated species in the 920-1080  $\text{cm}^{-1}$  region as shown below (Figure 5).

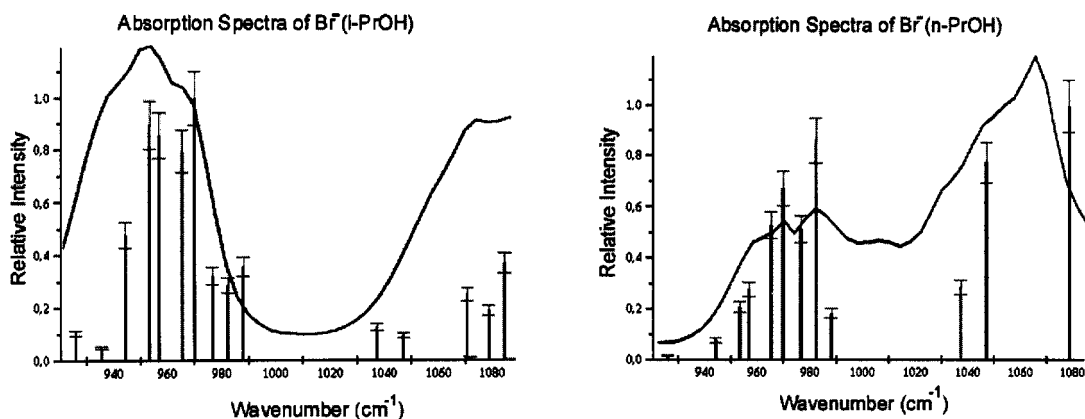


Figure 5: Absorption IR spectra of gas-phase  $\text{Br}^-(i\text{-ProH})$  and  $\text{Br}^-(n\text{-ProH})$  measured by the photodissociation yield as a function of the  $\text{CO}_2$  laser wavelength. The full envelope represents the normal IR spectra of the gaseous solvent molecules.

The spectra shown above are very encouraging and suggest that the combination of tunable IR lasers with ions trapped in the ICR cell can provide a unique way to obtain IR spectra of cluster ions.

## ACKNOWLEDGEMENTS

Our work has been generously supported by the São Paulo Science Foundation (FAPESP) through several grants and graduate and undergraduate student fellowships. We also acknowledge the support of the Brazilian Research Council (CNPq) in the form of a Senior Research Fellowship and graduate student support. Finally, most of this work would have not been possible without the technical help from Jair J. Menegon.

## REFERENCES

1. For a recent review of ion cyclotron resonance techniques and their applications, see T. Dienes, S. J. Pastor, S. Schlürch, J. R. Scott, J. Yao, S. Cui, C. L. Wilkins. *Mass Spectrom. Rev.* **15**, 163 (1996).
2. J. M. Farrar, W. H. Saunders, Jr. *Techniques for the Study of Ion-Molecule Reactions*, Wiley-Interscience: New York, 1988.
3. Y. Yang, H. V. Linnert, J. M. Riveros, K. R. Williams, J. R. Eyler. *J. Phys. Chem. A* **101**, 2371 (1997).
4. H. V. Linnert, J. M. Riveros. *Int. J. Mass Spectrom. Ion Processes* **140**, 163 (1994).
5. (a) D. Thölmann; D. S. Tonner, T. B. McMahon. *J. Phys. Chem.* **98**, 2002 (1994). (b) M. Sena, J. M. Riveros. *Rapid Comm. Mass Spectrom.* **8**, 1031 (1994). (c) P. D. Schnier, W. D. Price, R. A. Jockusch, E. R. Williams. *J. Am. Chem. Soc.* **118**, 7178 (1996).
6. R. C. Dunbar, T. B. McMahon. *Science* **279**, 194 (1998).
7. R. C. Dunbar, *J. Phys. Chem.* **98**, 8705 (1994).
8. M. Sena, J. M. Riveros. *J. Phys. Chem. A* **101**, 4384 (1997).
9. (a) G. T. Uechi, R. C. Dunbar. *J. Chem. Phys.* **96**, 8897 (1992). (b) T. Baer, O. Dutuit, H. Mestdagh, C. Rolando. *J. Phys. Chem.* **92**, 5674 (1988).
10. (a) T. Gaumann, Z. Zhu, M. C. Kida, J. M. Riveros. *J. Am. Soc. Mass Spectrom.* **2**, 372 (1991). (b) N. H. Morgon, H. V. Linnert, T. Giroldo, J. M. Riveros. *J. Phys. Chem.* **100**, 18048 (1996).
11. (a) M. L. Chabiny, S. L. Craig, C. K. Regan, J. I. Brauman. *Science* **279**, 1882 (1998). (b) W. L. Hase. *Science* **266**, 998 (1994); (c) J. M. Riveros, S. M. Jose, K. Takashima. *Adv. Phys. Org. Chem.* **21**, 197 (1985).
12. C. H. DePuy, S. Gronert, A. Mulin, V. M. Bierbaum. *J. Am. Chem. Soc.* **112**, 8650 (1990).
13. J.F.G. Faigle, P.C. Isolani, J.M. Riveros. *J. Am. Chem. Soc.* **98**, 2049 (1976).
14. H. Wang, W. L. Hase. *J. Am. Chem. Soc.* **119**, 3093 (1997).
15. K. Takashima, J.M. Riveros. *J. Am. Chem. Soc.* **100**, 6128 (1978).
16. M. L. P. da Silva, J. M. Riveros. *J. Mass Spectrom.* **30**, 733 (1995).
17. N. H. Morgon, A. B. Argenton, M. L. P. da Silva, J. M. Riveros. *J. Am. Chem. Soc.* **119**, 1708 (1997).
18. P. Kebarle, W. R. Davidson, J. Sunner, S. Meza-Höja. *Pure Appl. Chem.* **51**, 63 (1979).
19. (a) L.K. Blair, P.C. Isolani, J.M. Riveros. *J. Am. Chem. Soc.* **95**, 1057 (1973). (b) J.M. Riveros, A.C. Breda, L.K. Blair. *J. Am. Chem. Soc.* **95**, 4066 (1973). (c) J. M. Riveros, S. Ingemann, N. M. M. Nibbering. *J. Am. Chem. Soc.* **113**, 1053 (1991).
20. A. T. Blades, J. S. Klassen, P. Kebarle. *J. Am. Chem. Soc.* **117**, 10563 (1995).
21. (a) J. W. Larson, T. B. McMahon. *J. Am. Chem. Soc.* **105**, 2944 (1983). (b) J. W. Larson, T. B. McMahon. *J. Am. Chem. Soc.* **106**, 517 (1984).
22. K. Hiraoka, S. Mizuse. *Chem. Phys.* **118**, 457 (1987).
23. F. K. J. Tanabe, N.H. Morgon, J. M. Riveros. *J. Phys. Chem.* **100**, 2862 (1996).
24. A. A. Viggiano, S. T. Arnold, R. A. Morris. *Int. Rev. Phys. Chem.* **17**, 147 (1998).
25. J. V. Seeley, R. A. Morris, A. A. Viggiano. *J. Phys. Chem. A* **101**, 4598 (1997).
26. S.T. Arnold, A.A. Viggiano. *J. Phys. Chem. A* **101**, 2859 (1997).
27. (a) J. H. Choi, K. T. Kuwata, Y.B. Cao, M. Okumura. *J. Phys. Chem. A* **102**, 503 (1998). (b) P. Ayotte, C. G. Bailey, G. H. Weddle, M. A. Johnson. *J. Phys. Chem. A* **102**, 3067 (1998).